PART IV

LINE FORMATION IN EXPANDING ATMOSPHERES

LINE FORMATION IN EXPANDING ATMOSPHERES

(*Review Paper*)

D. G. HUMMER*

Joint Institute for Laboratory Astrophysics, National Bureau of Standards and University of Colorado, Boulder, Colo., U.S.A.

Abstract. The current state of understanding of line formation processes in expanding atmospheres is reviewed, and the successes and limitations of current computational techniques are summarized. Some results for differential rotation are also given, although very little work has been done in this area. Special attention is given to the severe difficulties that are encountered in inferring the structure of rapidly expanding or rotating atmospheres from observed line profiles because of the failure under these conditions of the Eddington-Barbier relation in integrated light; the value in this respect of continuum and interferometric observations is emphasized.

1. Introduction

The purpose of this review is to summarize our current understanding of radiative transfer and line formation processes in expanding atmospheres and to indicate the status of theory and computational development in this area. Because very little work has been done on the effects of differential rotation, primary emphasis is given to situations in which the gas flows radially outward; much of the discussion is also relevant to situations in which the gas flows inward. Limitations of space force us to ignore work on optically thin atmospheres despite its historical importance; these essentially geometrical arguments have been instrumental in the determination of the basic structure of the object we are considering, and are included naturally in the most recent computational techniques. It is hoped that this effort will be useful as an introduction to the field for the nonspecialist and as a guide to the literature. Although bibliographic completeness was not the primary consideration, the coverage is quite comprehensive.

It is convenient to consider separately low-velocity flows, in which the dispersion in flow speeds is less than or on the order of the mean thermal speed, and high-velocity flows, which involve speeds much larger than thermal; these cases are discussed in Sections 2 and 3, respectively. Although the important physical processes are the same for both cases, the useful phenomenological descriptions and the computational procedures are very different. The basic ideas of line formation in expanding atmospheres are clearly and completely discussed by Rybicki (1970), who also includes significant original work. Readers unfamiliar with the modern ideas of line formation in static atmospheres may find helpful the brief review by Hummer and Rybicki (1971b).

1.1. NOTATIONAL PRELIMINARIES

Throughout this review $v(r)$ or $v(\tau)$ is used for the radial velocity law, which is here always regarded as known; following the convention of most theoretical work in this

* Staff Member, Laboratory Astrophysics Division, National Bureau of Standards and Department of Physics and Astrophysics, University of Colorado.

area, v is taken to be positive for motion *towards* an observer situated outside the atmosphere. It is convenient to introduce the mean thermal speed of an atom of mass M at a typical temperature T,

$$v_{th} = \sqrt{2kT/M}, \tag{1.1}$$

as the unit of velocity, and to define

$$u = v/v_{th}. \tag{1.2}$$

The frequency displacement from the line center frequency ν_0 is conveniently measured in thermal Doppler units corresponding to v_{th}:

$$x = (\nu - \nu_0)/\Delta_0, \tag{1.3}$$

where

$$\Delta_0 = \nu_0 v_{th}/c. \tag{1.4}$$

A subtle point arises in the use of the variable x in transforming between inertial frames according to the well-known first-order Doppler formula

$$\nu^c = \nu^s(1 - \mu v/c), \tag{1.5}$$

where ν^s is the frequency of a photon measured in the frame of the stationary observer and ν^c is the frequency in a frame moving with a component of velocity $v\mu$ in the photon's direction of propagation; (below we shall identify the latter frame with the frame co-moving with the gas). If the definition (1.3) is applied consistently in each frame, i.e. $\tilde{x}^c \equiv (\nu^c - \nu_0^c)/\Delta_0^c$, then $\tilde{x}^c = x^s$. It is customary and more useful to define

$$x^c \equiv \frac{\nu^c - \nu_0^c}{\Delta_0^c}, \qquad x^s \equiv \frac{\nu^s - \nu_0^c}{\Delta_0^c} \tag{1.6}$$

with the result that, to first order in v/c,

$$x^c = x^s - u\mu; \tag{1.7}$$

this result is valid as well when Δ_0^c in (1.6) is replaced by Δ_0^s.

The depth in the atmosphere will be measured on the *mean* optical depth scale τ, which is related to the geometrical depth z by

$$d\tau = k\,dz, \tag{1.8}$$

where

$$k = (N_1 B_{12} - N_2 B_{21})h\nu_0/4\pi\,\Delta_0 \tag{1.9}$$

is the integrated line opacity. This definition is unaffected by the velocity field. For finite slabs the optical thickness on the τ-scale is represented by T.

2. Low Velocity Flows

When the maximum flow speed is less than a few times the mean thermal speed and the gradient is small, the most important effect of the velocity field is to distort the

monochromatic optical depth scale. The monochromatic optical depth $\tau_{x,\mu}$ of a layer at mean depth τ, measured from the surface of a planar atmosphere for specified values of the frequency x and the direction cosine μ is

$$\tau_{x,\mu}(\tau) = \mu^{-1} \int_0^\tau d\tau' \, \phi[x - \mu u(\tau')], \tag{2.1}$$

which, for a Doppler profile and a linear velocity law

$$u = u_0 + u_1\tau, \tag{2.2}$$

can be readily evaluated in terms of the error function. The Eddington-Barbier relation states that emergent intensity for specified x and μ is approximately equal to the source function at the mean optical depth $\tau = \tau^*(x, \mu)$ for which the monochromatic optical depth is unity, i.e. where $\tau^*(x, \mu)$ is the solution of

$$\tau_{x,\mu}(\tau) = 1. \tag{2.3}$$

We give, in Table I, values of $\tau^*(x, \mu = 1)$ for $u_0 = 0$ and $u_1 \geq 0$. As changing the sign of u leads simply to a change in sign of x, and giving u_0 a non-zero value is equivalent to replacing x by $x - \mu u_o$, it is sufficient for the present purpose to consider these cases in which the velocity vanishes at the surface (although in reality the flow vanishes below some point in the atmosphere).

We see from Table I that the effect of a positive velocity with a positive gradient (i.e. flow decelerating outward) is to redistribute the line opacity so that the longward side of the line is more transparent than the shortward side (also more transparent than in a static atmosphere). This implies that if the source function increases inwards for a sufficient distance, as in a normal stellar atmosphere, the radiation emerging on the longward side will be more intense than on the shortward side, so that an emission line will appear skewed to the red and an absorption line will be stronger in the blue. However, numerical calculations with $u = 0.01\tau$ and $S(\tau) = \tau$ yield an emission line with the blue component much stronger than the red; the Eddington-Barbier relation holds in the region of the line core and out to about $x = 5$, but fails completely in the red wing. Conditions for the validity of the Eddington-Barbier relations and alternative expressions valid at all frequencies are given by Hummer and Kunasz (1976).

Atmospheres with the flow accelerating outwards have been investigated numerically, using a realistic line-formation theory, by Hummer and Rybicki (1968a, b) for plane slabs of finite thickness and by Magnan (1968) and Mathis (1968) for expanding spherical atmospheres using Monte Carlo techniques and Λ-iteration, respectively. For optical thickness of order 50 and gradients of order $u_1 \simeq -0.1$, the ratio of red to blue peak heights was of order 1.5. In these cases the Eddington-Barbier relation appears to be fairly reliable. Although Magnan (1968) found that radiation from the receding hemisphere strengthened the red component, Hummer and Rybicki (1968b) showed that this skewing to the red was not caused primarily by receding material by considering a model in which the rear half of the slab was at rest, and the front half expanding. The explanation given above for the behavior of

D. G. HUMMER

TABLE I

Values of $\tau^*(x)$ for frequency x in the red (r) and blue (b) sides of the lines at which the monochromatic optical depth $\tau_x(\tau) = 1$ for velocity laws $u(\tau) = u_1\tau$. Here $\mu = 1$. Dashes indicate that the equation $\tau_x[\tau^*(x)] = 1$ has no solution, i.e. that any atmosphere is optically thin at these frequencies.

u_1		0	0.25	0.50	0.75	1.0	1.25	1.50	1.75	2.00	2.25	2.50
0.0		1.772	1.887	2.276	3.111	4.818	8.456	1.68+1	3.790+1	9.677+1	2.800+2	9.181+2
0.01	r	1.773	1.896	2.303	3.187	5.071	9.530	2.394+1	–	–	–	–
	b	1.773	1.878	2.251	3.041	4.603	7.685	1.369+1	2.452+1	4.115+1	6.239+1	8.604+1
0.03	r	1.774	1.916	2.361	3.363	5.748	1.454+1	–	–	–	–	–
	b	1.774	1.862	2.205	2.919	4.254	6.625	1.052+1	1.612+1	2.312+1	3.092+1	3.907+1
0.10	r	1.791	2.009	2.647	4.532	–	–	–	–	–	–	–
	b	1.791	1.823	2.079	2.606	3.491	4.815	6.583	8.700	1.103+1	1.347+1	1.595+1
0.30	r	1.984	2.795	–	–	–	–	–	–	–	–	–
	b	1.984	1.817	1.902	2.171	2.605	3.185	3.877	4.642	5.446	6.269	7.099

|x|

absorption and emission lines in low-speed flows was apparently first given by Hummer and Rybicki (1968a).

It is interesting to contrast this behavior with that when no gradient exists, as for example, when a geometrically thin spherical shell of gas expands with a *constant* velocity. Then both absorption and emission lines in the *flux* as seen by a distant observer at rest with respect to the center of the star are blue shifted. This simple consequence of the angular dependence of the Doppler formula (1.5) holds, of course, for both large and small velocities. Underhill (1947) applied this transformation to discrete-ordinate solutions of the static plane-parallel Schuster problem visualized as a thin spherical shell, and obtained a blue-shifted absorption profile with a strong red wing extending nearly to the red edge of the static profile.

Although small velocity fields can have quite profound effects on the emergent radiation field, the line source function is affected very little. The contrasting behavior of the emerging radiation and the internal excitation is shown dramatically in Figures 1 and 2, which represent the line source function and the flux profiles
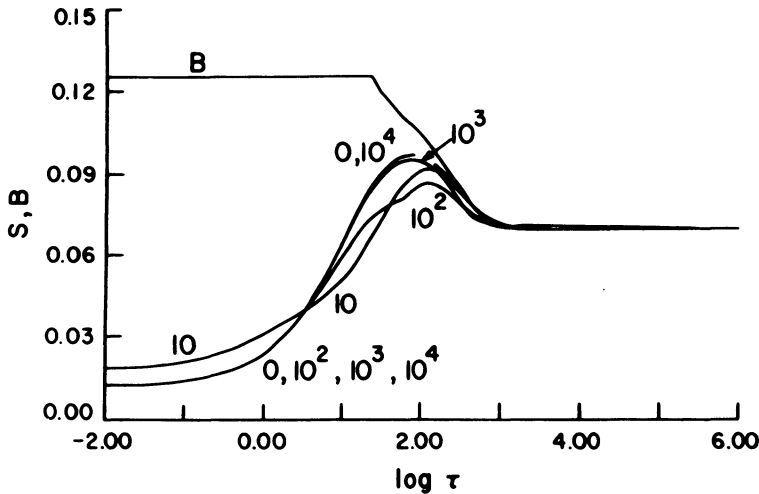
Fig. 1.   Planck functions and line source functions for $\varepsilon = 10^{-2}$ and $u(\tau) = 10/(1 + \tau/T)$, $T = 10, 10^2, 10^3$, 10^4. The static case is labeled by 0 (from Kalkofen, 1970).

calculated by Kalkofen (1970) for a semi-infinite planar atmosphere with the velocity law $u(\tau) = 10(1 + \tau/T)^{-1}$, where the parameter T has the values $10, 10^2, 10^3, 10^4$. The temperature is taken to be constant below $\tau = 10^3$; above that point it increases to give the Planck function shown in Figure 1. In many situations the source function is sufficiently insensitive to the velocity field that it may be calculated in a static approximation; only in calculating the emergent radiation field must the flow be taken into account.

This weak dependence of the source function on the flow is readily explained. The shift of line opacity from the core to the shortward side of the line does not reduce the core opacity enough to allow significant flux to be carried there, and the effect of impeding the flow of radiation in one wing is not serious so long as radiation can
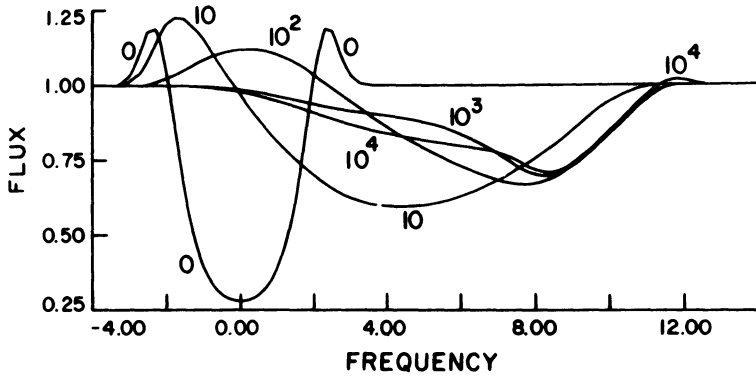
Fig. 2.   The emergent monochromatic flux corresponding to source functions in Figure 2. The frequency is measured from line center in thermal Doppler units (from Kalkofen, 1970).
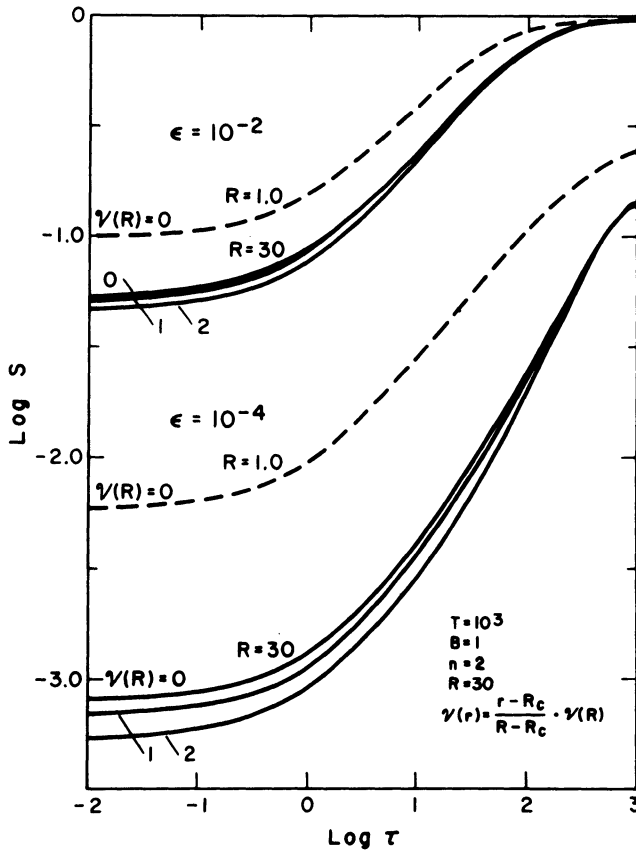
Fig. 3.   Line source functions for $R = 30$, $T = 10^3$, $B = 1$, $k(r) = kr^{-2}$ and a linear velocity law. Curves are labeled by $V(r) = [u(r)$ in text]. Broken lines given corresponding plane-parallel static limits (from Kunasz and Hummer, 1974b).

escape freely in the other wing; consequently the photoexcitation of the line-forming atoms is not substantially altered. Generally, the degree of excitation is slightly reduced for the static values, although in situations in which the velocity field is confined to the surface layers, the excitation is increased because of photoexcitation by the continuum. When the line opacity is spread from the core into both wings, either by thermal gradients, as first discussed by Hummer and Rybicki (1966) and Rybicki and Hummer (1967), or by non-monotonic velocity fields, as considered by Shine and Oster (1973), the source functions at depth can be quite large compared to the isothermal or static values, respectively.

The source function appears to be more sensitive to the geometry of the atmosphere than to its velocity field, at least for velocities less than a few times v_{th}. Figure 3, taken from Kunasz and Hummer (1974b), contrasts the line source functions for an internally excited (by electron collisions, for example) spherical shell with inner and outer radii of 1 and 30, respectively, with the source function for a planar slab of the same optical thickness ($T = 10^3$); in both cases a velocity linear in radius is assumed. The sensitivity to both the geometry and the flow increases as $\varepsilon \approx C_{21}/A_{21}$ decreases, i.e. as the effect of collisions decreases. In spherical geometry a velocity field $v(r)$ also induces a transverse gradient $v(r)/r$ in addition to the radial gradient dv/dr, which facilitates the escape of photons from deep layers. This effect, which has no counterpart in planar atmospheres with flow normal to the surface, is illustrated nicely in Figures 9 and 10 of Kunasz and Hummer (1974), which also show the sensitivity of the flux profile to velocities as small as a few percent of v_{th}.

Rybicki (1970) makes the important distinction between the divergence of the rays of radiation and the divergence of the velocities in a spherical atmosphere. It is quite possible that the rays do not diverge appreciably in an atmosphere in which the velocities do. For example, in a thin spherical shell of radius R and thickness ΔR, where $\Delta R \ll R$, the divergence of the rays is unimportant, but if $v\,\Delta R/R$ is comparable with v_{th}, the lateral motion of two points at the same radius in the shell separated by a distance of order ΔR is clearly significant. In this case it is clearly necessary to allow for the transverse gradient although the usual condition for the plane-parallel treatment of the radiation is satisfied. Rybicki derives a novel form of the planar transfer equation that allows for the inclusion of the transverse gradient.

The effects of rotation, alone and combined with expansion, have been studied (in the low velocity limit) only by Magnan (1970), who used the Monte Carlo method. His results, for a disc with the outer radius four times the inner and an optical thickness of 50, are reproduced in Figure 4. The rotational speed at every radius is $5v_{th}$ and the expansion velocity, in units of v_{th}, labels the curves.

Before going on to discuss numerical techniques, it is worth mentioning a very special transfer problem for which the essential properties of the radiation field can be obtained by approximate analytical arguments. Kahn (1968) has investigated the $L\alpha$ radiation field in an ionized region surrounded by an expanding spherical shell of neutral hydrogen that acts as a partially reflective enclosure. He allows for the reddening of the radiation by scattering from the expanding shell and by scattering within the ionized region; the latter problem is reduced to one of diffusion type in frequency space. By further simple considerations of the leakage of photons through the expanding shell, Kahn shows that the photons escape almost entirely in the
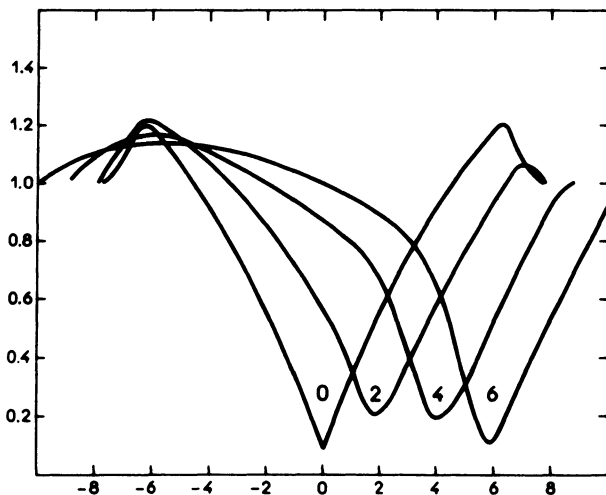
Fig. 4.   Flux profiles relative to continuum vs x for rotating disc with optical radius = 50, outer radius = 4 times the inner radius and rotational velocity of 5 thermal units at all radii. Curves are labelled by expansion velocity in thermal units (from Magnan, 1970).

extreme red wing of the line, with redshifts on the order of one percent of the line center frequency. He also discusses the effect of radiation pressure on the dynamics of the shell. Although these results were obtained in the context of planetary nebulae, the treatment appears to be applicable to the circumstellar region of hot stars.

2.1. NUMERICAL TECHNIQUES

For non-relativistic flow the transfer equation for a differentially moving atmosphere differs from that for the static case only in that the normalized profile of the line absorption coefficient $\phi(x)$ is replaced by $\phi(x - u\mu)$. Here μ is the cosine between the direction of propagation of radiation and the radius vector. Therefore most numerical differential equation techniques can be immediately applied to expanding atmospheres. The practical consequence of expansion is only that in differencing the transfer equation a wider range of frequencies and a large number of angle points must be used; the resulting system of linear algebraic equations can become extremely large, especially in extended atmospheres where the outward peaking of the radiation field necessitates a very fine angular mesh. In the solution of this system, two types of procedures – so-called elimination schemes – are in use, each with its advantages and disadvantages. We digress briefly to describe these schemes.

2.1.1. Elimination Schemes

The difference equations are ultimately to be solved for a quantity $y_{\gamma, d} = y(x_i, \mu_j, \tau_d)$, $\gamma = (i, j)$, $\gamma = 1, 2, \ldots, F$, $d = 1, 2, \ldots, N_1$ related to the radiation field with frequency x_i, direction cosine μ_j and optical depth τ_d; F and N are the total number of frequency-angle points and depth points, respectively. In the scheme

introduced by Feautrier (1964) the quantities $y_{\gamma,d}$ are organized into vectors labelled by the index d, in which the components are labeled by γ:

$$\mathbf{y}_d \equiv (y_{1d}, y_{2d}, \ldots, y_{Nd}), \qquad d = 1, 2, \ldots, N. \tag{2.4}$$

Rybicki (1971) recognized that in cases for which the number F of frequency-angle points is very large, it is advantageous to use the alternative arrangement

$$\mathbf{y}_\gamma = (y_{\gamma 1}, y_{\gamma 2}, \ldots, y_{\gamma N}) \qquad \gamma = 1, 2, \ldots, F ; \tag{2.5}$$

however this scheme can be used only if the line source function is independent of frequency and angle, i.e. depends on y only through a combination of the form

$$J_d = \sum_{\gamma=1}^{F} W_\gamma y_{\gamma d}, \tag{2.6}$$

where the quantities W_j are known constants. Estimates of the number of multiplications and divisions, and of the required storage space in the fast core, are given in Table II; the quantities C, C' and C'' are constants. The superiority of the Rybicki scheme in dealing with large numbers of frequency-angle points is clear.

TABLE II
Comparison of elimination scheme

	Feautrier	Rybicki
Operations	CNF^3	$C'N^2F + C''N^3$
Storage	NF^3	$2N^2$

2.1.2. Variable Eddington Factors

Variable Eddington factors, defined as the ratios of certain angular moments of the radiation field, provide the basis for an alternative strategy for cases in which the number F of frequency-angle points is very large, and the dependence of the line source function on the radiation field is more complex than (2.6). Although this procedure does not require angular discretization, so that F is simply the number of frequency points, it does call for a rapidly-convergent iterative process. This procedure was applied to static problems in planar geometry by Auer and Mihalas (1970) and to continuum and static-line problems in spherical atmospheres by Hummer and Rybicki (1971b) and Kunasz and Hummer (1974a), respectively. In this latter work the integrating factor introduced by Auer (1971) is essential.

2.1.3. Differential Equation Solutions

The earliest numerical solutions were those of Chandrasekhar (1945a, b), who solved the plane-parallel Schuster problem and the planetary nebula Lyman-α problem in an expanding slab; the techniques used in this work have provided the basis for much of the work on high velocity flow and will be discussed further in Section 3.0. Abhyankar (1964a, b, 1965, 1967) retained Chandrasekhar's assumptions of monochromatic scattering and a two-stream (Eddington approximation), but

by using an iterative technique based on transmission and reflection functions for thin layers derived from the transfer equation, he was able to treat more general velocity laws than Chandrasekhar and to use a Doppler profile. Kulander (1967) considered internally-excited atmospheres and used a generalization of the discrete-ordinate method to treat complete frequency redistributions, but was restricted to piece-wise constant velocity laws. In a subsequent paper, Kulander (1968) treated linear expansion by a method based on the superposition of basic solutions of the transfer equations regarded as a one-point boundary problem; the well-known instability of this approach limited him to relatively thin layers. Mathis (1968) used the slowly-convergent Λ-iteration method, but included partial redistribution and assumed spherical geometry. All of these techniques are now primarily of historical interest.

Most of the current work is based on a generalization of the method devised by Feautrier (1964), of which the elimination scheme has just been mentioned. Although this method is ideally suited for use with small velocity flows, and apparently had been so used by L. Auer in unpublished work as early as 1967, the first published results using complete frequency redistribution and internal excitation are those of Hummer and Rybicki (1968), who used the non-linear Riccati method. Kulander (1971) also used this technique to treat a large number of schematic models. The Feautrier method has proved superior to the Riccati method, however, and has been used extensively by many authors in studying moving atmospheres, including Rees (1970), Vardavas (1974), and Cannon and Vardavas (1974). In the latter two papers angle-averaged redistribution functions are used; the results will be discussed in Section 3.5. Cannon and Cram (1974) have generalized the Feautrier procedure further to account for the advection of material in high-speed flows, and Cannon (1974), in considering the propagation of pulses through an atmosphere, has introduced the conservation equations of gas dynamics into the Feautrier procedure. Cannon and Rees (1971) have developed a version of the Feautrier method to treat two-dimensional transfer in the presence of a two-dimensional velocity field; recent developments, including the use of Rybicki-type elimination, allow this problem to be solved much more efficiently (D. Mihalas, private communication). All of the above work has been restricted to planar geometries and has employed Feautrier elimination in solving the linear algebraic system obtained by differencing the transfer equation. Kunasz and Hummer (1974b) obtained solutions to the line transfer problem in expanding (or contracting) spherical atmospheres using the Rybicki elimination scheme.

2.1.4. *Integral Equation Solutions*

Much less work has been done using the integral form of the transfer equation, probably because the generalization of the standard techniques to allow for angle-dependent line opacities is less simple than for the differential equations. The integral equation methods are attractive because they scale like the Rybicki elimination scheme. Kalkofen (1970) has carried out the necessary generalization for expanding planar atmospheres and obtained the results presented above in Figures 2 and 3, for $u_{max} = 10$. This work illustrated clearly the necessity of using a large

number of angular points when $v_{th} \gtrsim 1$. For a spherical atmosphere expanding with the law $v(r) = \text{const} \cdot r$, the integral equation takes an especially simple form, which has been exploited by Robbins (1968) to solve the transfer problem including angle-averaged redistribution (cf. Section 3.5) for lines in the helium triplet system.

3. High Velocity Flows

In situations where the flow speeds are much larger than the mean thermal speed, it seems reasonable that the gross features of the radiation field in lines will be established by the macroscopic flow field, while the details are determined by the thermal motion of the atoms. This separation of roles has been exploited in the development of a very useful approximate theory, to be discussed below; of equal importance is the phenomenological picture of the line formation process to which it leads. Moreover, there are important conceptual and computational advantages in describing radiative transfer from the point of view of an observer in the co-moving frame of the gas, rather than from that of an external observer in a stationary frame at rest with respect to the center of the star. The frequency displacement x^s of a photon seen in the stationary frame is related to that in the co-moving frame x^c as given above by Equation (1.7).

As we here suppose that $v \gg v_{th}$, let us assume for the moment that photons are emitted only at line center in the co-moving frame, i.e. with $x^c = 0$. Then all photons seen in the stationary frame with a specified frequency x^s are emitted from surfaces on which

$$u(r)\mu = x^s,$$

i.e. the so-called 'constant velocity surfaces' on which the line-of-sight component of velocity has the value x^s. In Figure 5 appear some constant velocity surfaces for
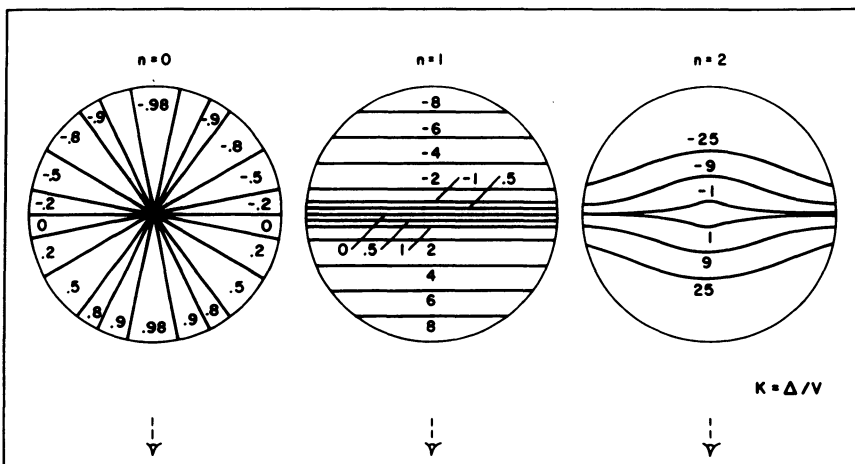
Fig. 5. Typical constant velocity surfaces for $u = u_0 (r/r_0)^n$, labeled by x/u_0. Line of sight is vertical from bottom of figure.

spherical atmospheres in which $u(r) = u_0(r/r_0)^n$, $r > r_0$; $n = 0, 1, 2$; here $r_0 = 1$ and the outer radius is $10\,r_0$. The curves are labelled with the value of (x/u_0).

It is clear at once that a given surface will extend over a non-zero range of radii, Δr, so that there is no way of knowing at what depth radiation with a specific frequency is formed. The familiar Eddington-Barbier relation, which is so ingrained in our thoughts, is now quite inapplicable. Consequently it is *in principle* impossible to infer the depth dependence of quantities such as temperature and density from observed line profiles with a resolution smaller than Δr. Moreover this situation implies that modeling will be severely nonunique. Because the location of the surface is independent of all opacity considerations, no additional information is obtained by using lines of varying strengths. Of course, the state of ionization and excitation will vary with the radius, so that the emission of a particular line *could* be confined to a relatively narrow range of radii, i.e. small compared to r; in other words only those parts of the surface that actually contain ions in the correct state will in fact contribute to the observed line profile.

In order to disentangle the atmospheric structure from the effects of the large-scale velocity field it is most helpful to use continuum observations over a very wide spectral range to infer the gross features of the atmosphere. Unfortunately this approach is at present hampered by the necessity of making large reddening corrections with sufficient accuracy to uncover intrinsic effects on the order of 0.01 mag. The advent of new and increasingly powerful interferometric techniques,
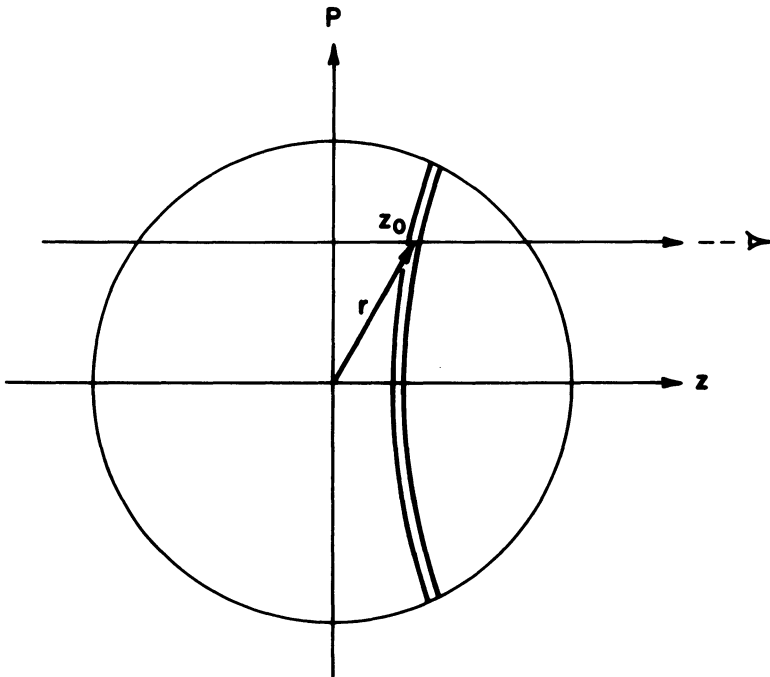
Fig. 6. Intersection of line of sight with constant velocity surface.

such as speckle and intensity interferometry, promises additional vital information. To capitalize on these innovations, it is essential in all modeling efforts to calculate quantities of interest such as limb-darkening laws and effective disc sizes for a wide range of frequencies.

Unfortunately, not all velocity laws lead to constant velocity surfaces that intersect any line of sight only once, as in Figure 6. Then radiation of a given frequency seen along a given line of sight comes from all of its intersections with the surface and the problem of inferring atmospheric structures from the profile is more difficult than ever. Even worse, from the theoretical point of view, is the fact that the regions around the points of intersection 'see' one another, so that the conditions of excitation at quite different radii are radiatively coupled. It is readily apparent that surfaces intersecting each line of sight uniquely are obtained if the velocity and its radial derivative are both positive, or both negative, throughout the atmosphere. In Figure 7 typical surfaces are shown for two velocity laws that violate these conditions, $u(r) = u_0(r/r_0)^{-1}$ and $u(r) = u_0[(r/r_0) - 2]$.
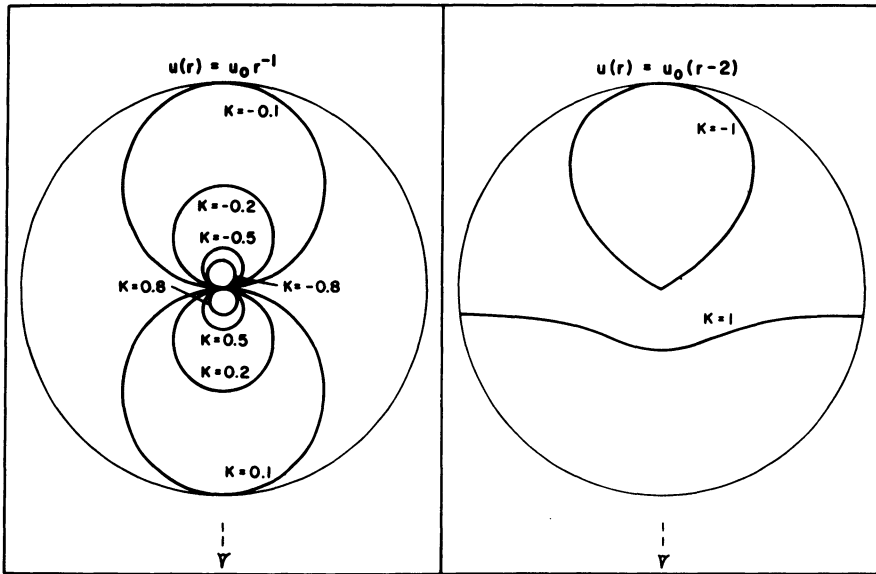
Fig. 7.   Typical constant velocity surfaces for $u = u_0(r/r_0)^{-1}$ and $u = u_0(r-2)$. Line of sight is vertical from bottom of figure.

Because the thermal speeds are not strictly zero, each constant velocity surface is more accurately thought of as a rather fuzzy thin shell with a geometrical thickness along a line of sight given essentially by the ratio of the mean thermal speed to the macroscopic velocity gradient in that direction. The corresponding optical thickness is the geometrical thickness times the total integrated line opacity per Doppler width, i.e., the quantity k defined by Equation (1.9). If we now consider a given line of sight intersecting a shell corresponding to a specific frequency, as illustrated in Figure 6, we see that the emissivity, as well as the opacity, at that frequency is accumulated

only within the shell. Mathematically, the optical depth and the emergent intensity are expressed by integrals over a Gaussian function of $x - u\mu$, where $u \gg 1$. To a very good approximation the only contribution to the integral comes from the region where the argument of the Gaussian is zero, i.e., in the shell.

One consequence of this localization of opacity and emissivity is that the transfer problem is confined to the shell. Although the optical depth of the shell is not necessarily small, it is finite, even in an atmosphere extending to infinity in three dimensions. In other words, the velocity field has induced in the atmosphere an *intrinsic escape process* for photons. When the probability of escape arising from the velocity field is sufficiently large, a very great simplification of the line transfer problem results; this fact is the basis of the so-called Escape Probability Method (EPM) which has been so useful in recent years.

3.1. THE ESCAPE PROBABILITY METHOD

Although the escape probability can be calculated in several ways, perhaps the simplest is a direct generalization of the derivation given by Zanstra (1949) for the static case; see Rybicki (1970) for details. For a line of integrated opacity k in a spherical atmosphere expanding with speed $u(r)$, the total optical depth along a line of sight for a photon of frequency x, in the observer's frame, is

$$\tau_x = \int_{-\infty}^{\infty} dz \, k(z)\phi[x - u(z)\mu(z)] \,, \tag{3.1}$$

where z is the distance along the line of sight. Changing the variable of integration to $x' = x - u(z)\mu(z)$ and accounting for the transverse and radial components of the velocity gradient, we have

$$\tau_x = \frac{k}{|f(\mu)|} \int_{-\infty}^{x} \phi(x') \, dx' \,, \tag{3.2}$$

where we have evaluated $k(z)$ and

$$f(\mu) = \mu^2 u'(r) + (1 - \mu^2)u(r)/r \tag{3.3}$$

on the appropriate constant velocity surface, i.e., where ϕ reaches its maximum. The probability that a photon emitted in the frequency interval $x, x + dx$ and in the element of solid angle $d\Omega$ escapes without further scattering is

$$\frac{1}{4\pi} d\Omega \, dx\phi(x) \exp(-\tau_x) \tag{3.4}$$

and summing over all frequencies and directions, we find for the net escape probability

$$\beta(r) = \frac{1}{k} \int_{0}^{1} f(\mu)[1 - \exp(-1/f(\mu))] \, d\mu \,; \tag{3.5}$$

the corresponding result for planar geometry is obtained by using $f(\mu) = \mu^2 u'(r)$. Thus the escape probability at radius r is a function only of the velocity and its radial derivative, and of the integrated line opacity. In deriving the expression (3.5) we

neglected the probability that the photon would strike the core. This effect is included in another escape probability β_c which is important in treating the interception of photons by the core; β_c is given approximately by $W\beta$, where W is the dilution factor at radius r. By applying the foregoing localization arguments to the exact expression for $\bar{J}$, the mean intensity integrated over the line profile factor $\phi(x)$, which enters the radiation rates in the statistical equilibrium equation, one obtains

$$\bar{J} = (1 - \beta)S(r) + \beta_c I_c, \qquad (3.6)$$

where I_c is the intensity in the photospheric continuum near the line and $S(r)$ is the line source function. Then $\bar{J}$ can be eliminated using the equation of statistical equilibrium, which for the two-level model atom is

$$S = (1 - \varepsilon)\bar{J} + \varepsilon B. \qquad (3.7)$$

Here ε is the probability per scattering that a photon is lost from the line by collisional de-excitation and B is the Planck function at ν_0 for the local electron temperatures. The resulting expression for $S(r)$ can be inserted in the usual expressions for the emergent flux profile.

For a semi-infinite isothermal planar atmosphere with a constant gradient (in τ),

$$\gamma \equiv du/d\tau = \text{const}, \qquad (3.8)$$

the exact surface value of the source function is readily shown to be

$$S(0) = \varepsilon B/\sqrt{\varepsilon + \beta - \varepsilon\beta}; \qquad (3.9)$$

here β is the escape probability (3.5) specialized to the planar case. This result, which contrasts explicitly the two mechanisms of velocity-induced photon escape and photon destruction by collisional de-excitation was implied by Rybicki (1970) and derived explicitly by Magnan (1974a), who also obtained the exact reflection coefficient for the same model. Frisch and Frisch (1975) gave an expression for the mean number of scatterings for a photon escaping from the same model atmosphere; they too derive the value of the surface source function.

3.1.1. *Development and Applications of the EPM*

The EPM was systematically developed by Sobolev (1947, 1952, 1957), who used it to study recombination and other spectra where the emissivity, as obtained by solving the equations of statistical equilibrium, was either independent of depth or varied in a simple known manner. Subsequent applications by Rublev (1961, 1964) and Lyong (1967) involved a variety of *ad hoc* assumptions concerning the distribution of emissivity. The present state of the theory, in which the emissivity at every point is determined by a self-consistent solution of the equations of statistical equilibrium, is due to Castor (1970), Rybicki (1970), and Lucy (1971). Castor and Rybicki both work from the integral forms of the transfer equation and assume complete redistribution in the co-moving frame; Castor gives explicit expressions for all quantities involved for the case of spherical geometry, while Rybicki presents a more discursive treatment, which includes the derivation of the escape probability

from several points of view and is applicable to an arbitrary geometry and flow field. Lucy, on the other hand, bases his treatment on the differential form of the transfer equation and carries out his development primarily on the assumption of coherent scattering in the co-moving frame, although he briefly considers complete redistribution in the fluid frame; he quotes numerical results indicating that the difference between the two assumptions is completely negligible. Lucy's transfer equation, which describes the migration of the photon in frequency space at a fixed depth, has been studied in detail by Noerdlinger and Scargle (1972), using the method of addition of layers. Hewitt and Noerdlinger (1974) have discussed the case of a doublet, in which blue absorption features of one component overlap the other component.

Castor and Van Blerkom (1970) have applied the EPM to a 30-level He II ion and Castor and Nussbaumer (1972) have treated a 14-level C III ion, both in the context of a spherical Wolf-Rayet star. Kuan and Kuhi (1975) have used a 12-level hydrogen atom in their work on Balmer line profiles in P Cygni. The EPM has also been used extensively (although not always correctly) in calculating the cooling of interstellar clouds, for which inward motion is usually important.

It is important to note that the EPM, as presently developed, is limited to velocity laws for which the velocity surfaces intersect every line of sight not more than once, i.e. it can be used only for accelerating outflow or decelerating inflow. Although Kuan and Kuhi (1975) account for the contribution of multiple intersections with the line of sight, they ignore, without comment, the radiative coupling between the regions in the vicinity of the points of intersection. When the restriction to unique interactions is heeded and only thermal Doppler broadening is present in the co-moving frame, i.e. when natural and collisional broadening is unimportant, the EPM is accurate for a wide range of conditions; both Castor (1970) and Rybicki (1970) discuss in some detail error estimates and conditions for validity. It follows from Equation (12) of Castor (1970), that if the profile function $\phi(x)$ has Lorentz wings of any non-zero strength, the first omitted term diverges, so that the EPM is invalid in this case. If at the base of the flow the velocity gradient is too small for the EPM to be valid, Lucy (1971) points out that it can still be used with the understanding that the resultant profile within a few thermal Doppler widths of line center will be inaccurate. Finally, because the EPM in its present form takes no account of the static part of the escape probability, i.e. the escape probability in a static atmosphere that is usually negligible with respect to the velocity-induced-escape, it gives source functions that are too large near open boundaries when the static term becomes important.

The EPM can also be applied to more complicated geometries than those with spherical symmetry; Rybicki's (1970) general expressions have already been mentioned. For the study of Be stars, combined differential rotation and expansion in a cylindrically symmetrical configuration is of special interest. One immediate difficulty is that the constant velocity surfaces, at least for pure rotation with reasonable velocity laws, intersect the line of sight more than once. The intersections of typical surfaces with the equatorial plane for $u_{\text{tan}} = u_0(r/r_0)^n$, $n = 0, 1, 2$, are very similar to the curves appearing in Figure 6 viewed from the side of the figure. Although this is merely a complicating factor if the source function is assumed or known a priori, as in

the case considered by Sobolev (1947), it poses a severe problem as discussed above for a self-consistent solution. Fortunately, it appears that differential rotation imposed on rapid expansion leads to tractable surfaces.

Current work on radiation-driven stellar winds (Lucy and Solomon, 1970; Castor *et al.*, 1975) depends crucially on evaluating the force of radiation in a spectral line on a volume of gas in a rapidly expanding atmosphere. Using the EPM, Sobolev (1957) found an expression for the force arising from the diffuse radiation generated in the envelope. In a thorough study relating the line forces to the atmospheric parameters Castor (1974) showed that the force arising from the photospheric continuum in conditions typical of early-type and Wolf-Rayet stars strongly dominated the force from the diffuse field. Castor's expression provided the basis for the Castor *et al.* (1975) theory of stellar winds.

3.2. ACCURATE NUMERICAL SOLUTIONS

We now turn to numerical procedures for the solution of the line transfer equation that can be used for high-velocity flows without making the approximations of the EPM. The transformation to the co-moving frame has already been discussed in connection with the velocity surfaces. This idea, which seems to have been introduced by Milne (1930) appears in the earliest consideration of transfer in moving media (McCrea and Mitra, 1936) and was first exploited in a systematic way by Chandrasekhar (1945a). Rottenberg (1952) also used this transformation in an interesting way. By regarding the extended atmospheres as a small number of geometrically thin shells, although with arbitrary optical thicknesses, he derived two coupled integral equations that could be solved easily by integrating from blue to red. Although he assumed only constant expansion velocities, he did obtain realistic profiles.

There are several reasons for the great utility of transformation to the frequency in the co-moving frame. Consider the scattering integral for an expanding atmosphere as it appears in the stationary frame:

$$\bar{J} = \int_{-\infty}^{\infty} dx \int_{-1}^{1} d\mu \, \phi(x - u\mu) I(x, \mu) . \tag{3.10}$$

In an atmosphere where the maximum velocity in thermal units is u_{max}, the intensity $I(x, \mu)$ contributes substantially to the integral over an interval of length approximately $2u_{max}$; for the static case, or in the co-moving frame the length of the interval is of order five. As u_{max} can be of order 10^3 in stellar winds the use of the co-moving frame offers an enormous advantage. As the angle of the ray changes slightly in the stationary frame, the line opacity profile $\phi(x - u\mu)$ and hence the intensity will change drastically, so that a very fine mesh of μ-points (and consequently of x-points) is required to represent the radiation field and to evaluate the scattering integral. As will be discussed below it is possible to use the so-called angle-averaged redistribution function in the co-moving frame when the presence of strong natural broadening wings prohibits the use of complete frequency redistribution; in the stationary frame this approximation is worthless.

The advantages of working in the co-moving frame are not without cost. The

emergent radiation field in the observers frame must be obtained by a separate calculation which is straightforward in principle but troublesome in practice. From the form of the transfer equation in the co-moving frame an even more important fact is apparent. For spherical geometry we have

$$\mu \frac{\partial I}{\partial r}(\nu, \mu, r) + \frac{1-\mu^2}{r} \frac{\partial}{\partial \mu} I(\nu, \mu, r) - \frac{\nu_0}{c}\left[\mu^2\frac{dv}{dr} + (1-\mu^2)v/r\right]\frac{\partial}{\partial \nu}I(\nu, \mu, r)$$
$$= \eta(\nu, r) - \chi(\nu, r)I(\nu, \mu, r),$$
(3.11)

where χ is the opacity and η the emissivity which in general depends on an angle and frequency integration over $I(\nu, \mu, r)$. In the stationary frame the term in $dI/d\nu$ is absent, so that the equation can be integrated as an *ordinary* differential equation on the characteristics of the differential operator, which are simply the rays parallel to any diameter. When the frequency derivative is present, it is necessary to treat equation (3.11) as a *partial* differential equation.

Before discussing the integration of Equation (3.11), a few comments on its form are appropriate. The term in $\partial I/\partial \nu$, which arises from the transformation to the co-moving frame, contains both radial and tranverse velocity gradients. Although the term is of formal order v/c, relative to the remaining terms, two other terms of the same order that arise from advection and aberration are ignored. Because of the presence of the large number ν_0 in the $\partial I/\partial \nu$ term, it is really of order v/v_{th} relative to the advection and aberration terms, as may be seen by writing the frequency in Doppler units (this was pointed out to us by Dr G. B. Rybicki). A recent study of the effect of these small terms by Mihalas *et al.* (1976b) shows that they lead to effects of order $5(v/c)$ in the source function; fortunately these occur sufficiently close to the surface that their effect on the emergent flux profile is negligible under stellar wind conditions. Although the Equation (3.10) has been known for a long time, problems concerning the correct form of the angle-moment equations derived from it and its use in connection with the gas dynamical equations have been resolved definitively by Castor (1972). Haisch (1976) has derived an alternative expression in tensor form for the transfer equation in the co-moving frame, which leads directly to a stable and conservative differencing scheme in any coordinate system.

As the transfer equation is now a partial differential equation, initial conditions in frequency space must be properly specified for the problem to be well-posed. In addition the differencing schemes in depth and frequency must be chosen, keeping stability criteria in mind. Under the conditions $v \geq 0$, $dv/dr \geq 0$, i.e. the same conditions necessary for unique velocity surfaces, all points recede from one another. Consequently radiation at any point appears redder than at the point where it was emitted. In particular as the extreme shortward edge of the line receives only reddened continuum radiation, the initial condition in frequency space is simply that the line intensity there is continuous with the adjacent continuum intensity at all depths. The frequency and elimination then proceeds from blue to red, as in Rottenberg's (1952) method. Obviously if $v \leq 0$, $dv/dr \leq 0$, all points approach one another and the initial condition is placed in the red wing. If v and dv/dr do not everywhere have the same sign, the frequency integration is more difficult, and will be discussed briefly below.

The first satisfactory solution of the co-moving frame equation was obtained by Noerdlinger and Rybicki (1974) for plane parallel geometry, using Feautrier elimination. Their procedure has proved to be fast, efficient and stable for a wide variety of velocity laws and atmospheric models. A similar procedure, with a slightly different elimination scheme that offers some advantages has been developed by Mihalas *et al.* (1976d), who described modifications necessary to treat non-monotonic velocity fields. An earlier method developed by Simonneau (1973) for plane geometry used co-moving frequencies in the context of an integral equation approach, but is restricted to linear velocity laws with small gradients.

Recently, two different solutions of the co-moving frame transfer equation in spherical geometry have been obtained by Mihalas *et al.* (1975, 1976c). The first method uses Rybicki elimination and is capable of handling very extended atmospheres and arbitrarily large velocity fields, but requires the assumption of complete frequency redistribution in the fluid frame. The second method employs variable Eddington factors (cf. 2.1.2) to eliminate angle quadratures, so that Feautrier elimination is practicable. This scheme allows the use of more accurate descriptions of the scattering in the co-moving frame; unfortunately, both of these solutions require that v and dv/dr have the same sign everywhere.

At present all of the published work on the co-moving frame transfer equation is restricted to two-level atoms. However, Mihalas, Kunasz and Hummer (unpublished) have formulated a multi-level solution using Rybicki elimination and the complete-linearization technique of Auer and Mihalas (1969); coding is now underway.

3.3. TYPICAL RESULTS FOR EXPANDING SPHERICAL ATMOSPHERES

A number of the more important effects of high velocity flow in a self-excited spherical atmosphere have been studied by Mihalas *et al.* (1975). In these models, electron scattering is treated by an assumption of complete redistribution so that the electron scattering opacity and emissivity are approximated by $n_e\sigma_e$ and $n_e\sigma_eJ_c$, respectively, where J_c is the mean intensity in the adjacent continuum. The optical depth in the line and continuum are 10^3 and 2, respectively, and the probability per scattering of collisional de-excitation is $\varepsilon = 2 \times 10^{-3}$. The line, continuum and electron-scattering opacity are proportional to r^{-2}, and a velocity law of the form

$$v(r) = v_{max}[\tan^{-1}(ar+b) - \tan^{-1}(a+b)] \tag{3.12}$$

was chosen to represent a velocity field which increases rapidly at any prechosen radius. The outer radius R has a value of either 3, 30 or 300 times the radius R_c of the core, at which a diffusion boundary condition was applied. Results for some isothermal models are shown in Figure 8. The source functions are labeled by v_{max} in thermal units; the broken lines represent the mean continuum intensity J_c, obtained by a solution of the continuum transfer equation. In these examples the velocity gradient reaches its maximum at $r \simeq (R+1)/2$. At large depths, the velocity gradient causes the escape probability to increase, so that the source function approaches J_c, which for the cases considered here lies below the source function deep in the
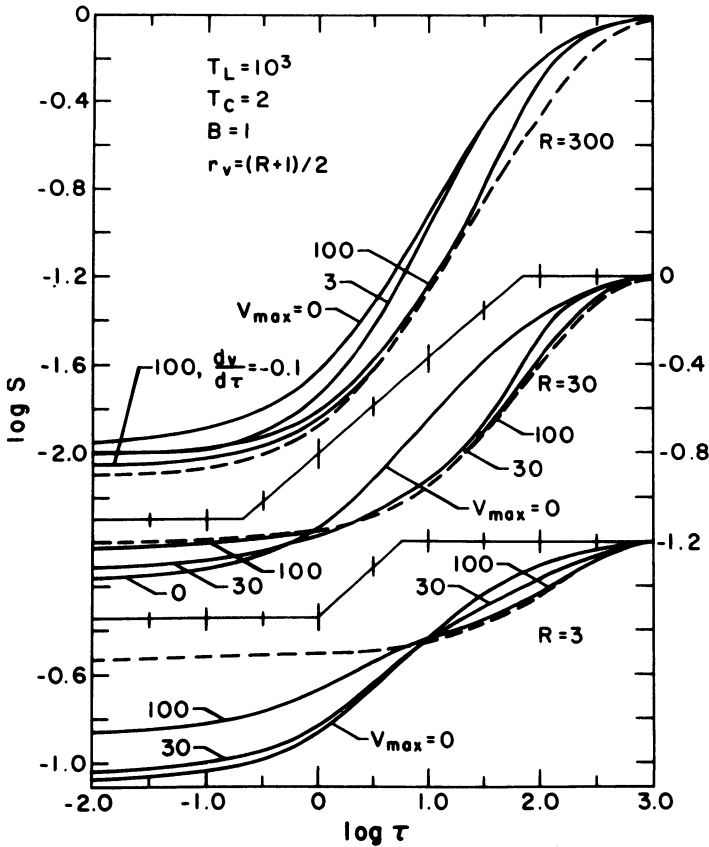
Fig. 8. Line source function vs line optical depth for isothermal models with various values of R and u_{max}. For each value of R the continuum mean intensity J_c is drawn as a broken line. For $R = 300$ an additional source function is included for $u_{max} = 100$ and $du/d\tau = 0.1$ (from Mihalas *et al.*, 1975).

atmosphere. This effect is largest for small R because the velocity gradient corresponding to a given value of v_{max} is steepest in this case.

In the outer layers the velocity gradient again causes the escape probability to increase, but also causes the line to intercept continuum photons; again the line source function approaches J_c but because, for small R, J_c ($\sim R^{-2}$) is relatively large, the source functions near the surface *increase* with v_{max}. When R is very large, J_c becomes quite small in the outer layers because of electron scattering and dilution, and the source function falls as v_{max} increases. The sensitivity of the source function to the form of the velocity law is illustrated in the top panel of Figure 8 by the case $v_{max} = 100$, $dv/d\tau = -0.1$, where the enhanced escape probability at all depths causes the source functions to be even closer to J_c than for the velocity law (3.12).

In Figure 9, the corresponding flux profiles in the observer's frame are given. The flux is normalized to unity in the continuum and is plotted as a function of the frequency displacement from line center in units of a scale factor x_{max} because of the extreme widths of the profiles. The scale factors x_{max} depend on R and v_{max} and are
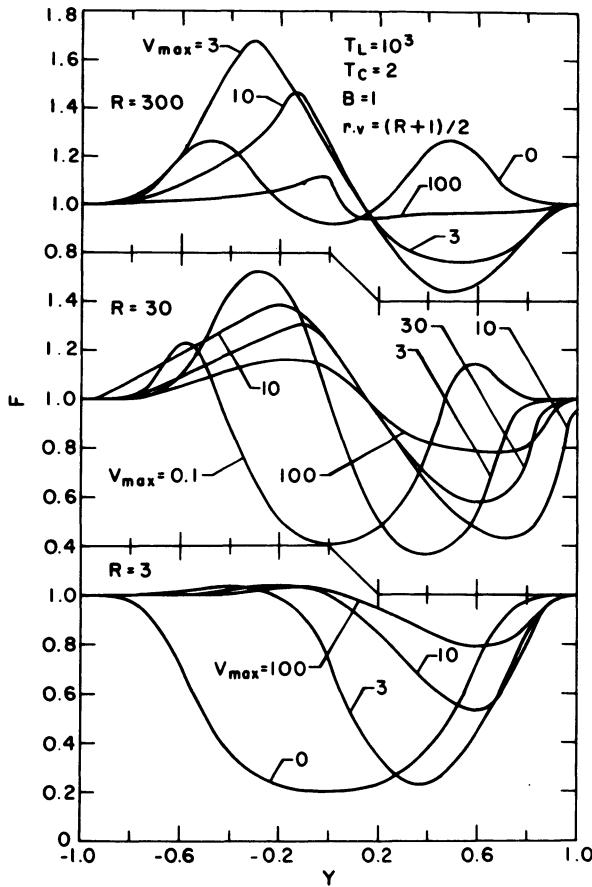
Fig. 9.   Emergent fluxes relative to the continuum for some functions of Figure 9 vs displacement
$y = x/x_{max}$, where values of x_{max} are listed in Table 2 (from Mihalas *et al.*, 1975).

TABLE III

Scale factors x_{max}

v_{max}	$R = 3$	$R = 30$	$R = 300$
0	3.0	3.5	3.5
3	5.5	6.0	4.5
10	13.0	11.0	12.0
30	–	35.0	–
100	100.0	100.0	100.0

given in Table III. For $R = 3$, there is not enough extension for significant emission, but the shortward shift of the absorption feature is clearly variable. There is also an increase in the absorption equivalent width, which in real spectra with non-zero noise might be confused with 'microturbulence'. In the more extended atmospheres, strong emission lines appear with large blue absorption troughs; as v_{max} increases, the peaks move to shorter wavelengths, while the minima initially move shortward

before reversing direction. The peaks assume a distinctive symmetrical triangular shape. For the largest velocities the features become quite indistinct.

For the moderately extended atmospheres with $R = 30$ and $v_{max} = 10$ in the above sequence, the limb-darkening curves are plotted in Figure 10, because of their potential importance for interferometry. It is clear here that limb darkening is very much more severe than in static planar cores because of the geometrical extension; moreover, as a consequence of the velocity field, the disc of the star exhibits bright rings when viewed in the near line wings.
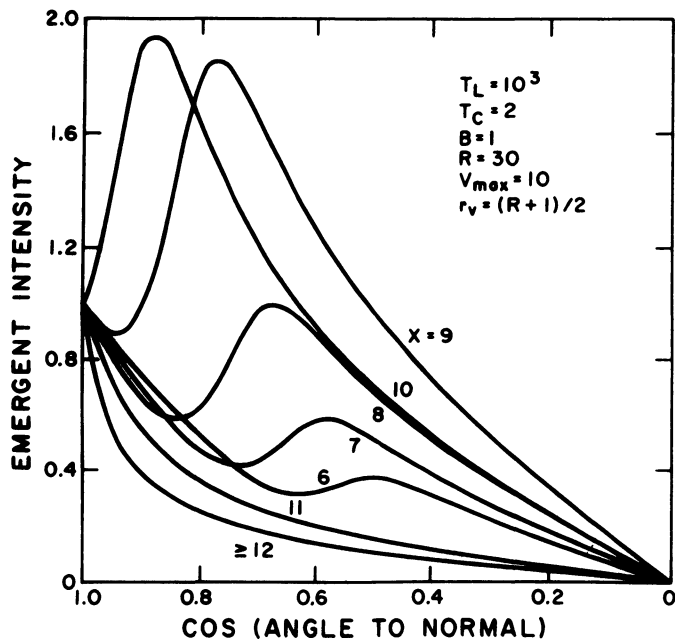
Fig. 10. Limb-darkening curves normalized to unity at $\mu = 1$ vs μ, for various displacements x from line center, for model with indicated parameters ($V_{max} = u_{max}$ in text and r_v is radius at which velocity gradient is largest) (from Mihalas *et al.*, 1975).

3.4. The temperature distribution in an expanding atmosphere

To examine in a highly idealized way the effects of a large velocity field on the temperature structure of the atmosphere, Mihalas *et al.* (1976a) have calculated radiative-equilibrium picket-fence models of expanding, spherical atmospheres, in which the run of density and velocity are specified *a priori*. Of particular interest were the heating and cooling arising from the shift of line opacity into the continuum, and from the enhanced photon escape rate, respectively. As is well known, the effect in a static atmosphere of introducing a line into the continuum is to lower the temperature at the surface, while raising it at depth ('backwarming'); as deviations from LTE increase, the surface effect becomes quite small. In expanding atmospheres, it is useful to think in terms of three mechanisms that influence the temperature structure: (a) the *irradiation effect*, in which surface layers are heated by intercepted

continuum radiation; (b) *band-width constriction*, in which the line opacity shifted to the wings impedes photon escape and causes heating in the deeper layers; and (c) *escape enhancement*, which can lead to cooling deep in the atmospheres if large velocity gradients are present there. An example of this effect is seen in the temperature drop at a velocity discontinuity, as obtained, for example, in the schematic models of Mihalas (1969). The first two effects are clearly seen in Figure 11, where the Planck function is plotted against the continuum optical depth for
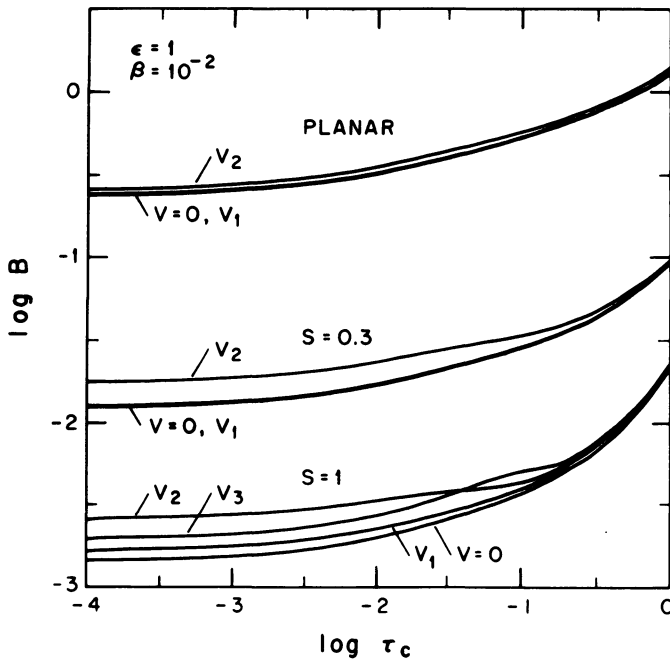
Fig. 11. Picket fence models for static and expanding atmospheres with $\varepsilon = 1$, $\beta = 10^{-2}$ and various velocity laws with $u_{max} = 12$; $V = 0$ is static case; V_1 designates constant velocity gradient; V_2 and V_3 designate case with sharp rise at line optical depth of 1 and 10, respectively.

moderately strong lines that cover approximately 0.2 of the spectrum. These models range from planar to moderately extended, depending on the value of the parameter S, the ratio of the mean free path in the continuum at the outer boundary to the radius of the atmosphere. In all cases except $v = 0$, the maximum flow speed at the surface was $12\,v_{th}$. Curves labeled V_1 are for models with a constant value of dv/dr, while those marked V_2 and V_3 correspond to a sharp rise in flow speed at line optical depths of 1 and 10, respectively. As the lines depart further from LTE the effects are qualitatively the same, but become smaller in magnitude. When the speed is small at large depths and rises suddenly to v_{max} at line optical depth unity (case V_2) both the irradiation and bandwidth constriction effects are apparent; the boundary temperature is raised by 16% in the most favorable case. If the maximum gradient occurs near line optical depth of ten, local heating occurs but the distinction between the two effects is blurred.

Although these results are based on very simple models, they do show that velocity fields can lead to substantial modifications of the temperature distributions by purely radiative means, quite apart from any dissipation of mechanical energy. Such temperature modifications are large enough to influence significantly the dynamical processes occurring in the atmosphere.

3.5. THE QUESTION OF FREQUENCY REDISTRIBUTION

Nearly all of the work on line formation in static media in the past decade has been based on the assumption of complete frequency redistribution (CFR), in which the frequency and direction of a photon before and after scattering are completely uncorrelated. The corresponding emissivity of scattered radiation is proportional to

$$\phi(\nu) \int d\nu' \int d\mathbf{n}' \, \phi(\nu') I(\nu', \mathbf{n}') \,. \tag{3.13}$$

However, this approximation is the third in a hierarchy of approximations derived from the exact scattering term

$$\int d\nu' \int d\mathbf{n}' \, R(\nu, \mathbf{n}, \nu', \mathbf{n}') I(\nu', \mathbf{n}') \,, \tag{3.14}$$

where ν' and $\mathbf{n}'$ are the frequency and direction of the photon before scattering and $R(\nu, \mathbf{n}, \nu', \mathbf{n}')$ is the so-called redistribution function. The second level of approximation involves the assumption that the variation with direction of the radiation field is unimportant, so that the intensity $I(\nu', \mathbf{n}')$ can be replaced by its mean value $J(\nu')$, in which case the emissivity becomes

$$\int d\nu' \, R(\nu, \nu') J(\nu') \,, \tag{3.15}$$

where $R(\nu, \nu')$ is the angle-averaged redistribution function. The redistribution functions have been discussed in detail by Hummer (1962). The assumption of CFR can be justified when the radiation field is approximately isotropic and white near the line center, as was apparently first shown by Bieberman (1947) and Holstein (1947). Extensive numerical calculations by Hearn (1964), Hummer (1969), and Milkey and Mihalas (1973) have confirmed the validity of CFR for static media.

On the other hand, because the presence of a velocity field reduces the degree of both whiteness and isotropy of radiation in the lines, the validity of CFR in moving media must be reconsidered. Magnan (1968), on the basis of Monte Carlo calculations for a spherical shell expanding with a constant velocity of one thermal unit found very little difference between the exact scattering expression and CFR, applied in the co-moving frame. On the other hand Vardavas (1974) and Cannon and Vardavas (1974), working in the observer's frame and using an angle-averaged redistribution function due to Hummer (1968) that included the effect of the velocity field, found very large effects from CFR. Magnan (1974b) criticized the use of angle-averaged functions in the observer's frame for moving atmospheres. Mihalas *et al.* (1976d) repeated the calculations of Cannon and Vardavas, using both CFR and an angle-averaged redistribution function in the *co-moving* frame, and obtained

nearly identical line profiles. It appears that in the derivation of the angle-averaged redistribution function for moving atmospheres in the observer's frame, the flow velocity is treated as a random velocity that is averaged together with the thermal velocity; consequently the photons are distributed over much too wide a spectral region, at least for $v \gtrsim v_{th}$, and the resulting function is also independent of the direction of the flow.

Caroff *et al.* (1972) have made an extensive investigation of different redistribution mechanisms in a rapidly expanding spherical shell with large velocity gradients, using the Monte Carlo techniques in which they follow the history of individual photons emitted with a known frequency at the inner boundary. They considered three cases: (1) coherence in the atom's frame; (2) coherence in the co-moving frame; (3) complete redistribution in the co-moving frame. The first of these is identical to the use of the full redistribution function in the co-moving frame; the second was used extensively by Lucy (1971). Caroff *et al.* pointed out that the correlation between frequency and direction that is explicitly enforced when coherence in the atom's frame is assumed gives rise to a skewing of the profile of the emergent radiation to longer wavelengths. This effect, which is different from others so far discussed, can be understood with the aid of Figure 12. A photon of frequency ν_e emitted in the core
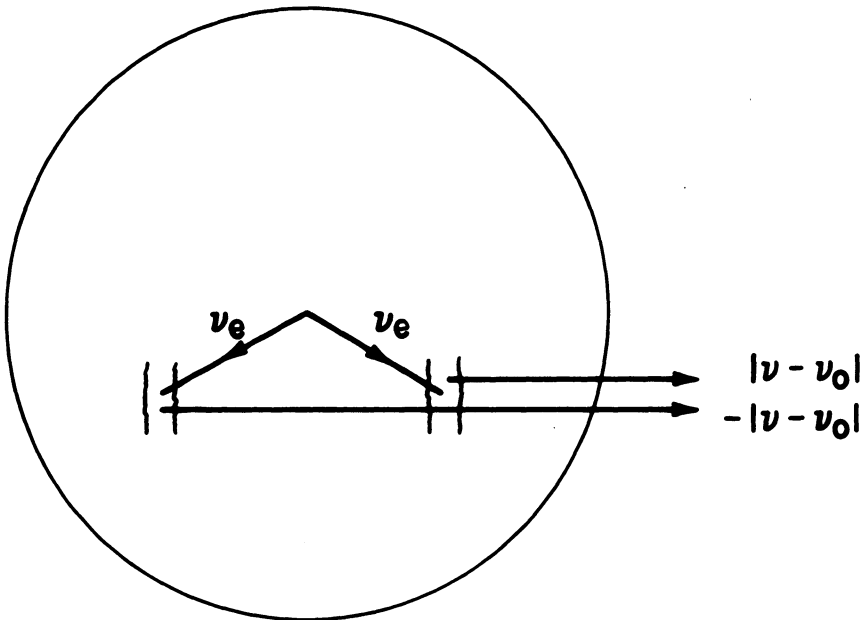
Fig. 12. Photons emitted with frequency ν_l are seen with frequency displacements $\pm |\nu - \nu_0|$.

and scattered from constant velocity surfaces symmetrically located in front and behind the core will be seen by the stationary observer with equal displacements from the line center ν_0. However, the photon with the shorter wavelength is seen slightly reddened by the atom in its constant velocity surface and has therefore a higher probability of being absorbed than has the longer wave photon, which has an

inward component of velocity as it travels through its shell. Occulation produces the opposite effect, however, and it is likely that in most cases of interest this is not a major effect. For high velocity flows it appears that the precise assumption about frequency redistribution in the co-moving frame is not of great consequence, so long as the thermal Doppler effect is the only important broadening mechanism. If natural broadening is significant, as in H I or He II $L\alpha$, and if the optical thickness is large enough for most of the transfer to occur in the wings, it is essential to use the appropriate angle-averaged redistribution function in the co-moving frame, just as for static problems. The numerical solutions of Mihalas *et al.* (1975) for expanding extended spherical atmospheres, using CFR, coherent scattering and angle-averaged redistribution functions for both pure Doppler and combined Doppler and natural broadening verify explicitly the above conclusions. This work shows also that the assumption of complete redistribution for *electron* scattering is valid for a wide range of conditions.

3.6. MATERIAL ADVECTION

For rapid flow, the equation of statistical equilibrium must contain terms accounting for the material carried into and out of the volume element under consideration, i.e. for material advection. Rybicki (1970) showed by essentially dimensional arguments that advection was negligible for resonance lines in Wolf-Rayet stars, although it could become significant for forbidden lines. Cannon and Cram (1974) derived an expression for the source function accounting for material advection of the form

$$S = (1-\varepsilon)\bar{J} + \varepsilon B - \frac{(1-\varepsilon)}{A_{21}}\frac{dS}{dt}, \tag{3.16}$$

where the last term, containing the time derivative of the source function following the fluid element, represents the effect of advection. In order to demonstrate the importance of the advection term, they solved numerically a model in which a wave with an amplitude of 2 km s^{-1} and a frequency in the kilocycle range travels upward through a medium at a speed of 0.2 km s^{-1}; the mean thermal speed is taken to be 1 km s^{-1}. The numerical solutions for the source function show deviations as large as 30 percent from the case where advection is neglected. Although one would expect the source function to be affected by this velocity field, it is unfortunately difficult to reconcile these results with simple estimates of the effect of advection. For their model one unit of optical depth corresponds to a geometrical distance of 10^{-4} km; on the other hand during the lifetime of 10^{-8} s assumed for the excited state of the atom, a typical distance it could move at the maximum velocity of particles in the wave is 10^{-8} s $\times$ 2 km s^{-1} = 2×10^{-8} km. Because the scale for advection is nearly four orders of magnitude smaller than the optical scale, it is difficult to understand how advection could have any appreciable effect in this case. It appears likely that their numerical integration, in which they used 1 second time steps to integrate a system with a relaxation time of order 10^{-8} s, may be at fault.

It is straightforward to derive from Cannon and Cram's expression explicit conditions that indicate when material advection can be neglected. For a macro-

scopic *steady* radial flow of speed $v(\tau)$, we can rewrite the Lagrangian time derivative of the source function as

$$\frac{dS}{dt} = \frac{dS}{d\tau}\frac{d\tau}{dt} = k\frac{dS}{d\tau}\frac{dz}{dt} = kv\frac{dS}{d\tau}, \tag{3.17}$$

where k is given by Equation (1.9). Using the well known relation among the Einstein coefficients, we find

$$\frac{(1-\varepsilon)}{A_{21}}\frac{dS}{dt} = \frac{(1-\varepsilon)}{8\pi} \quad N_1\lambda_0^3(\omega_2/\omega_1)(v/v_{\text{th}})(dS/d\tau), \tag{3.18}$$

where we have neglected the stimulated emission term in k. Here ω_1 and ω_2 are the statistical weights of the lower and upper levels respectively, N_1 is the density of the line-forming ion and λ_0 is the line-center wavelength (in centimeters). It is interesting that Equation (3.18) contains no reference to the radiative transition probability.

When $\varepsilon \ll 1$, as is the case for strong lines, the production of excited atoms near the outside of the atmospheres is controlled by radiation flowing up from great depths in the line wing rather than by thermal excitation, i.e. the $(1-\varepsilon)\bar{J}$ term is the controlling one and not εB. Although a precise statement of the proper magnitude for comparison involves rather elaborate arguments in terms of the thermalization length, it is sufficient for our purpose to compare the advection term with $(1-\varepsilon)\bar{J}$, or equivalently, with S. Thus the condition that advection is unimportant near the surface can be written as

$$\frac{v}{v_{\text{th}}} \ll \left(\frac{8\pi}{(1-\varepsilon)N_1\lambda_0^3}\right)\left(\frac{\omega_1}{\omega_2}\right)\left(\frac{S}{dS/d\tau}\right). \tag{3.19}$$

Now $S/(dS/d\tau)$ is very roughly approximated by τ; a better estimate can be obtained from Ivanov's (1973) approximate expression for the source function in a semi-infinite isothermal atmosphere:

$$S \simeq \sqrt{\varepsilon}B[\varepsilon + (1-\varepsilon)K_2(\tau)]^{-1/2}, \tag{3.20}$$

where

$$K_2(\tau) = \int_{-\infty}^{\infty} dx\,\phi(x)E_2[\tau\phi(x)] \tag{3.21}$$

is a function that decreases monotonically from $E_2(0) = 1$ *as* τ increases from 0. The desired result is

$$\frac{S}{dS/d\tau} \simeq \frac{\varepsilon + (1-\varepsilon)K_2(\tau)}{(1-\varepsilon)K_1(\tau)} \xrightarrow[K_2 \gg \varepsilon]{} K_2(\tau)/K_1(\tau), \tag{3.22}$$

where

$$K_1(\tau) = (-1/2)\,dK_2/d\tau; \tag{3.23}$$

the properties of K_1 and K_2 are discussed in detail by Avrett and Hummer (1965). For Doppler broadening $K_2/K_1 = 1.7$, 3.2 and 15 at $\tau = 0.1$, 1.0 and 10 respectively, and for Lorentz broadening these values should be increased by a factor of

approximately two. Thus at $\tau = 1$, the product of the last two factors in Equation (3.19) is roughly unity and for $\lambda_0 = 5000$ Å and $N_1 = 10^{10}$, which is typical of an abundant ion density in a stellar wind, the remaining factor is of order 2000.

Deep in the atmosphere, the advection term must be compared with the thermal excitation term εB. The last factor in (3.19) must therefore be replaced by $\varepsilon B/(dS/d\tau)$, which can be estimated in the same way. For $\varepsilon = 10^{-4}$ and $\tau = 10^3$, 10^4 and 10^5, this factor is approximately 0.5, 15 and 1300, respectively; for the values of N_1 and λ_0 used above and setting $\omega_1/\omega_2 = \frac{1}{3}$, the corresponding values for the right side of the condition (3.19) are roughly 300, 10^4 and 10^6.

From these arguments it appears that material advection in stellar winds is of at most marginal importance as far as the lines are concerned. However, as this conclusion is based on the model of a two-level atom, it is possible that the interplay of slow and fast rates could cause an observable effect.

3.7. ELECTRON SCATTERING

In regions where rapid flow occurs, the densities can become quite low and the material will be largely ionized. Consequently a significant density of electrons can be expected in the flow, which suggests that electron scattering could play a role in the line formation process. This problem was apparently considered by Edmonds (1950), but his treatment is based on a highly artificial separation of the electrons into a reversing layer.

The treatment of electron scattering on the same basis as scattering by line atoms is difficult, even for static situations, because the thermal Doppler width for the electrons is so much greater than that for the atoms. This problem has been attacked by Auer and Mihalas (1968a, b) and in a simplified way, by Weymann (1970) and Mathis (1970).

Auer and Van Blerkom (1972) have used the Monte Carlo technique to examine the scattering of photons by electrons in a spherical shell expanding with either a constant or a linear velocity law. They suppose that the photons are initially emitted as the result of recombination, but that the atoms do no scattering. They obtain results for electron optical thickness of 0 and 1 and for cases in which the thermal velocity of the electrons is either negligible compared to the flow velocity, or equal to its value at the inner boundary of the shell. For unit optical thickness they obtain emission lines with core widths in agreement with the flow velocities, but with very strong, extended red wings. The red wings are a consequence of the spherical distribution of the electrons, as can be seen in Figure 13. When a photon is scattered at radius r, the value of $\mu = \cos \theta$ is symmetrically distributed between about $\mu = 0$, so that $\langle \mu \rangle = 0$. If the next scattering occurs at a radius r_s that is larger than r, it makes an angle θ_s with the radius vectors such that $\mu_s = \cos \theta_s \geq \mu$. As the distribution of direction cosines in the case is biased towards 1, we have $\langle \mu_s \rangle > 0$. The direction cosine μ_s' after scattering is again symmetrically distributed and $\langle \mu_s' \rangle = 0$. If the thermal speed is small compared to the flow speed, the frequencies involved in the scattering at r_s are related by

$$x' - x = u(r_s)(\mu_s' - \mu_s) \,. \tag{3.24}$$
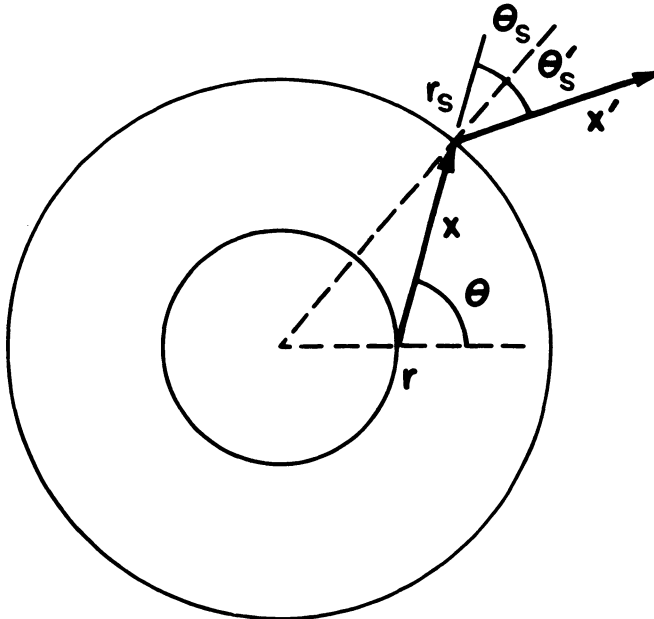
Fig. 13. Photons scattered at $r_s > r$ have $\langle \mu_s \rangle \ge 0$ and $\langle x' - x \rangle \le 0$.

Averaging over many events, we have

$$\langle x' - x \rangle = -u(r_s)\langle \mu_s \rangle , \tag{3.25}$$

so that the frequency shift is redward. Since the photons are flowing from smaller to larger radii, this reddening effect is preponderant. It appears that this effect is not restricted to optically thin lines; the fact that emission lines are not usually observed to have extended red wings may imply certain limits on the densities and dimensions of the expanding atmospheres in question.

4. Conclusion

At present an understanding of line formation and our computational ability to solve line transfer problems for accelerating radial flow in spherically symmetrical configurations are both well developed. As the computations are unfortunately extremely heavy and require the largest available computers, work in this area is now restricted to a comparatively small number of people. The treatment of line formation in cylindrically symmetrical flows by either the escape probability method or by direct numerical integration of the transfer equation is very much more difficult than for the spherical case, and little progress has been made. Even when accurate numerical solutions are available meaningful comparisons of model results with observed line profiles will be difficult because of the smearing of structural details by the line formation process in high-speed flows.

Acknowledgements

I am indebted to my friends and colleagues John Castor, Paul Kunasz, Dimitri Mihalas and George Rybicki for their patient assistance over the years in helping me to understand many of the ideas discussed here and for their comments on this review. I am grateful to Drs Wolfgang Kalkofen and Christian Magnan for permission to reproduce figures from their papers. The writing of this review has been supported in part by the National Science Foundation through Grant No. MPS72-05026 A02 to the University of Colorado.

References

Abhyankar, K. D.: 1964a, *Astrophys. J.* **140**, 1353.
Abhyankar, K. D.: 1964b, *Astrophys. J.* **140**, 1368.
Abhyankar, K. D.: 1965, *Astrophys. J.* **141**, 1056.
Abhyankar, K. D.: 1967, in M. Hack (ed.), *Modern Astrophysics, A Memorial to Otto Struve*, Gauthier-Villars, Paris, p. 199.
Auer, L. H.: 1971, *J. Quant. Spectrosc. Radiat. Transfer* **11**, 573.
Auer, L. H. and Mihalas, D.: 1968a, *Astrophys. J.* **153**, 245.
Auer, L. H. and Mihalas, D.: 1968b, *Astrophys. J.* **153**, 923.
Auer, L. H. and Mihalas, D.: 1969, *Astrophys. J.* **158**, 641.
Auer, L. H. and Mihalas, D.: 1970, *Monthly Notices Roy. Astron. Soc.* **149**, 65.
Auer, L. H. and Van Blerkom, D.: 1972, *Astrophys. J.* **178**, 175.
Avrett, E. H. and Hummer, D. G.: 1965, *Monthly Notices Roy. Astron. Soc.* **130**, 295.
Bieberman, L. M.: 1947, *J. Exp. Theor. Phys.* **17**, 416.
Cannon, C. J.: 1974, *J. Quant. Spectrosc. Radiat. Transfer* **14**, 745.
Cannon, C. J. and Cram, L. E.: 1974, *J. Quant. Spectrosc. Radiat. Transfer* **14**, 93.
Cannon, C. J. and Rees, D. E.: 1971, *Astrophys. J.* **169**, 157.
Cannon, C. J. and Vardavas, I. M.: 1974, *Astron Astrophys.* **32**, 85.
Caroff, L. J., Noerdlinger, P. D., and Scargle, J. D.: 1972, *Astrophys. J.* **176**, 439.
Castor, J. I.: 1970, *Monthly Notices Roy. Astron. Soc.* **149**, 111.
Castor, J. I.: 1972, *Astrophys. J.* **178**, 779.
Castor, J. I.: 1974, *Monthly Notices Roy. Astron. Soc.* **169**, 279.
Castor, J. I., Abbott, D. C., and Klein, R. I.: 1975, *Astrophys. J.* **195**, 157.
Castor, J. I. and Nussbaumer, H.: 1972, *Monthly Notices Roy. Astron. Soc.* **155**, 293.
Castor, J. I. and Van Blerkom, D.: 1970, *Astrophys. J.* **161**, 485.
Chandrasekhar, S.: 1945a, *Rev. Mod. Phys.* **17**, 138.
Chandrasekhar, S.: 1945b, *Astrophys. J.* **102**, 402.
Edmonds, F. N.: 1950, *Astrophys. J.* **112**, 324.
Feautrier, P.: 1964, *Compt. Rend.* **258**, 3189.
Frisch, U. and Frisch, H.: 1975, *Monthly Notices Roy. Astron. Soc.* **173**, 167.
Haisch, B. M.: 1976, *Astrophys. J.*, in press.
Hearn, A. H.: 1964, *Proc. Phys. Soc.* **84**, 11.
Hewitt, T. G. and Noerdlinger, P. D.: 1974, *Astrophys. J.* **188**, 315.
Holstein, T.: 1947, *Phys. Rev.* **72**, 1212.
Hummer, D. G.: 1962, *Monthly Notices Roy. Astron. Soc.* **125**, 21.
Hummer, D. G.: 1968, *Monthly Notices Roy. Astron. Soc.* **141**, 479.
Hummer, D. G.: 1969, *Monthly Notices Roy. Astron. Soc.* **145**, 95.
Hummer, D. G. and Kunasz, P. B.: 1976, to be published.
Hummer, D. G. and Rybicki, G. B.: 1966, *J. Quant. Spectrosc. Radiat. Transfer* **6**, 661.
Hummer, D. G. and Rybicki, G. B.: 1968a, *Astrophys. J.* **153**, L107.
Hummer, D. G. and Rybicki, G. B.: 1968b, in R. G. Athay, J. Mathis, and A. Skumanich (eds.), *Resonance Lines in Astrophysics*, National Center for Atmospheric Research, Boulder, Colorado, p. 213.
Hummer, D. G. and Rybicki, G. B.: 1971a, *Ann. Rev. Astron. Astrophys* **9**, 237.
Hummer, D. G. and Rybicki, G. B.: 1971b, *Monthly Notices Roy. Astron. Soc.* **152**, 1.
Ivanov, V. V.: 1973, in D. G. Hummer (ed.), *Transfer of Radiation in Spectral Lines*, NBS Spec. Publ. No. 385 (Washington: Govt. Printing Office), p. 441.

Kahn, F. D.: 1968, in D. E. Osterbrock and C. R. O'Dell (eds.), 'Planetary Nebulae', *IAU Symp.* **34**, 236.
Kalkofen, W.: 1970, in H. Groth and P. Wellmann (eds.), *Spectrum Formation in Stars with Steady-State Extended Atmospheres*, NBS Spec. Publ. No. 332 (Washington: Govt. Printing Office), p. 120.
Kuan, P. and Kuhi, L. V.: 1975, *Astrophys. J.* **199**, 148.
Kulander, J. L.: 1967, *Astrophys. J.* **147**, 1063.
Kulander, J. L.: 1968, *J. Quant. Spectrosc. Radiat. Transfer* **8**, 273.
Kulander, J. L.: 1971, *Astrophys. J.* **165**, 543.
Kunasz, P. B. and Hummer, D. G.: 1974a, *Monthly Notices Roy. Astron. Soc.* **166**, 19.
Kunasz, P. B. and Hummer, D. G.: 1974b, *Monthly Notices Roy. Astron. Soc.* **166**, 57.
Lucy, L. B.: 1971, *Astrophys. J.* **163**, 95.
Lucy, L. and Solomon, P. M.: 1970, *Astrophys. J.* **159**, 879.
Lyong, L. V.: 1967, *Soviet Astron.* **11**, 224.
Magnan, C.: 1968, *Astrophys. Letters* **2**, 213.
Magnan, C.: 1970, *J. Quant. Spectrosc. Radiat. Transfer* **10**, 1.
Magnan, C.: 1974a, *J. Quant. Spectrosc. Radiat. Transfer* **14**, 123.
Magnan, C.: 1974b, *Astron. Astrophys.* **35**, 233.
Mathis, J. S.: 1968, in R. G. Athay, J. Mathis, and A. Skumanich (eds.), *Resonance Lines in Astrophysics*, National Center for Atmospheric Research, Boulder, Colorado, p. 299.
Mathis, J. S.: 1970, *Astrophys. J.* **162**, 761.
McCrea, W. and Mitra, K.: 1936, *Z. Astrophys.* **11**, 359.
Mihalas, D.: 1969, *Astrophys. J.* **157**, 1363.
Mihalas, D., Kunasz, P. B., and Hummer, D. G.: 1975, *Astrophys. J.* **202**, 465.
Mihalas, D., Kunasz, P. B., and Hummer, D. G.: 1976a, *Astrophys. J.* **203**, 647.
Mihalas, D., Kunasz, P. B., and Hummer, D. G.: 1976b, *Astrophys. J.* in press.
Mihalas, D., Kunasz, P. B., and Hummer, D. G.: 1976c, *Astrophys. J.* in press.
Mihalas, D., Shine, R. A., Kunasz, P. B., and Hummer, D. G.: 1976d, *Astrophys. J.*, in press.
Milkey, R. W. and Mihalas, D.: 1973, *Astrophys. J.* **185**, 709.
Milne, E. A.: 1930, *Z. Astrophys.* **1**, 98.
Noerdlinger, P. D. and Rybicki, G. B.: 1974, *Astrophys. J.* **193**, 651.
Noerdlinger, P. D. and Scargle, J. D.: 1972, *Astrophys. J.* **176**, 463.
Rees, D. E.: 1970, *Proc. Astron. Soc. Australia* **1**, 384.
Robbins, R. R.: 1968, *Astrophys. J.* **151**, 511.
Rottenberg, J. A.: 1952, *Monthly Notices Roy. Astron. Soc.* **112**, 10.
Rublev, S. V.: 1961, *Soviet Astron.* **4**, 780.
Rublev, S. V.: 1964, *Soviet Astron.* **7**, 492.
Rybicki, G. B.: 1970, in H. Groth and P. Wellmann (eds.), *Spectrum Formation in Stars with Steady-State Extended Atmospheres*, NBS Spec. Publ. No. 332 (Washington: Govt. Printing Office), p. 87.
Rybicki, G. B.: 1971, *J. Quant. Spectrosc. Radiat. Transfer* **11**, 589.
Rybicki, G. B. and Hummer, D. G.: 1967, *Astrophys. J.* **150**, 607.
Shine, R. A. and Oster, L.: 1973, *Astron. Astrophys.* **29**, 7.
Simonneau, E.: 1973, *Astron. Astrophys.* **29**, 357.
Sobolev, V. V.: 1947, *Moving Envelopes of Stars*, Leningrad State University (in Russian), trans. S. Gaposchkin, Harvard University Press, Cambridge, Massachusetts (1960).
Sobolev, V. V.: 1952, in V. A. Ambartsumyan (ed.), *Theoretical Astrophysics* (in Russian), trans. J. B. Sykes, Pergamon Press, London (1958).
Sobolev, V. V.: 1957, *Soviet Astron.* **1**, 678.
Underhill, A. B.: 1947, *Astrophys. J.* **106**, 128.
Vardavas, I. M.: 1974, *J. Quant. Spectrosc. Radiat. Transfer* **14**, 909.
Weymann, R. J.: 1970, *Astrophys. J.* **160**, 31.
Zanstra, H.: 1949, *Bull. Astron. Inst. Neth.* **11**, 1.

DISCUSSION

Snijders: I agree with your comment that it is very difficult to get anything useful out of one or two lines, but what if you take a number of lines which have different excitation potentials and different ionization potentials, for example, Si II and Si IV, and combine this with N V, say?

Hummer: Clearly the more information you have the better off you are. However, a constant velocity surface encompasses a range of radius. If you have a lot of different stages of excitation you have emission

only in a relatively small radius band, and therefore that will help to isolate where on the surface you are. So if you have conditions where the degree of ionization changes rapidly, the depth resolution will be increased and lines of different ions will then give more information than just one line.

Kalkofen: One of your slides in which you compare the effects of velocity fields and geometry shows dramatic effects due to geometry. What was the ratio of the outer radius to the mean free path of photons?

Hummer: The radius is small relative to the mean free path of photons.